10th International Conference on
Steel and Aluminium Structures (ICSAS24)
Rio de Janeiro, Brazil, 5-7, June, 2024

CARRYING CAPACITY OF THIN-WALLED COLD-FORMED SQUARE HOLLOW COLUMNS WITH LARGE HOLES

Marios-Zois BEZAS[a], Maxime VERMEYLEN[a], Helene MORCH[b], Koenraad GINCKELS[c] and Jean-François DEMONCEAU[a]

[a] Steel and Composite Construction, UEE Research Unit, Liège University, Liège, Belgium
Emails: marios-zois.bezas@uliege.be, maxime.vermeylen@uliege.be, jfdemonceau@uliege.be

[b] GDTech, Belgium
Email: helene.morch@gdtech.eu

[c] Stow international, Belgium
Email: Koenraad.Ginckels@stow-group.com

Keywords: Hollow sections; Cross-section resistance; Buckling; EN1993-1-3; Thin-walled members.

Abstract. *Thin-walled cold-formed hollow columns are widely used in steel structure construction due to their advantages such as high strength, ductility and light weight. When bolted connections are realized, large holes may be used at the level of the connections in order to allow screwing the bolts and to avoid the use of long bolts along the width of the cross-section. This paper investigates the influence of these considerable holes on the resistance and stability of the column. More specifically, square hollow sections with large holes have been considered and their behaviour has been studied numerically using shell elements, accounting for both local and distortional effects, as well as material and geometrical non-linearities. The obtained results have been then compared with the predictions obtained through the code provisions for the cross-section resistance and member buckling.*

1 INTRODUCTION

Thin-walled cold-formed steel elements consists a very attractive structural solution due to their fast manufacturing and erection on-site, as well as their high strength and ductility combined with a light weight. These sections are extensively used as both primary or secondary structural elements in buildings, storage system structures or steel houses. The design of cold-formed steel structures is governed by two main problems: (a) the stability phenomena and (b) the connecting technology. The former is dominant for the design criteria while the latter seems to be quite specific and sometimes strongly affects the structural behaviour and the design details of these elements.

When hollow sections are used for the columns of these structures, the beams are usually welded to them, while in the case of bolted connections, long bolts all along the column's section width are required. An alternative solution could be that large holes are used at the level of the connections allowing thus the tightening of the bolts, that are significantly shorter, by hand. These bolts are common ones and can be found much easier than the longer ones that sometimes should be produced on demand, an aspect that increases both the time and the cost of the structure. In addition, by using long bolts, there is always the risk to provoke a local crash

on the column face, especially for thin-walled ones as covered in this study; the more the bolt is tightening in order to provide an adequate contact of the elements the more the risk of local failure on the column face is increasing. Besides that, for some countries, this joint configuration is not acceptable by their inspection committees. Therefore, the use of the handholes at the connection level's looks to be a good structural solution.

Although a lot of studies have been performed by various researchers, they are mainly focusing on gross hollow sections, i.e. without handholes. Toffolon et al. [1] studied experimentally and numerically the local and interactive buckling behaviour of gross hollow sections, and in [2], they were provide design recommendations for the buckling resistance of cold-formed SHS members. Yun et al. [3] and Li et al. [4] investigated the influence of the steel grade and of the residual stresses respectively on the resistance of square hollow sections. In the framework of the recently finished RFCS European project with the acronym HOLLOSSTAB [5] which involved numerical and experimental investigations, design rules and recommendations for the verification of the cross-sectional and member stability and strength of gross hollow sections of various shapes and steel grades have been provided. On the contrary, the research focusing on square hollow members with holes are very limited. Singh et al. [6] examined numerically the effects of various hole shapes (i.e. circular, square, hexagonal) and sizes on the buckling behaviour of cold-formed and hot-rolled steel stub columns. Devi at al. [7] studied experimentally and numerically the torsional behaviour of unperforated and fully perforated cold-formed steel square hollow section members.

The objective of this paper is to investigate the influence of the handholes on the column faces used for tightening the bolts at the level of the floors on the resistance and stability of the columns. To achieve this, a large number of parametrical numerical studies on SHS columns subjected to compression or compression and bending have been conducted with ABAQUS software [8] using shell elements. The results have been then compared with analytical ones obtained by applying the provisions of the existing codes. In Europe, the design of hollow thin-walled columns is carried out by using mainly EN 1993-1-3 [9] which is dedicated to the design cold-formed profiles, with references to EN 1993-1-1 [10] and EN 1993-1-5 [11] when relevant. Therefore, comparisons are made here with the resistances evaluated in accordance with EN 1993-1-3; references are also made to the provisions of its forthcoming version prEN 1993-1-3 [12] only when those differ from the provisions of the former. Finally, recommendations for the design of such structural elements are provided.

These studies are part of the ongoing project funded by SPW project entitled ACTIONS: "Advanced Eurocodes Compliant Tools for Industrial Optimized Innovative Structures", involving STOW group, GDTech and CRM companies, as well as the University of Liege.

2 FINITE ELEMENT MODELLING

All the numerical models for the parametrical numerical studies presented in this article were created with ABAQUS non-linear finite element software using isoparametric shell elements with reduced integration (i.e. type S4R). The samples have been modelled as pin – ended at their extremities at the centre of gravity of the gross section, where fictitious end plates have been introduced through a specific constraint, so as to distribute uniformly the external applied loads on the cross-section but also to avoid any local failure at the load application point (see Figure 1). In all simulations, the following two steps were applied. First, a linear buckling analysis (LBA) was performed in order to obtain both local and global elastic critical loads as well as their eigenshapes. These eigenshapes are then used, separately or combined, as initial imperfection shapes within the second simulation step, where a full non-linear analysis (GMNIA) was carried out in order to obtain the maximum load carrying capacity of the column;

in these simulations, the applied load is increasing up to failure. For all simulations the steel grade HX420LAD was set constant. An elastoplastic material behaviour law with strain hardening in accordance to EN 1993-1-5 has been adopted. In addition, based on the provisions of prEN 1993-1-3 [12] and EN 10346 [13], its basic yield strength is equal to f_{yb} = 400 N/mm^2.

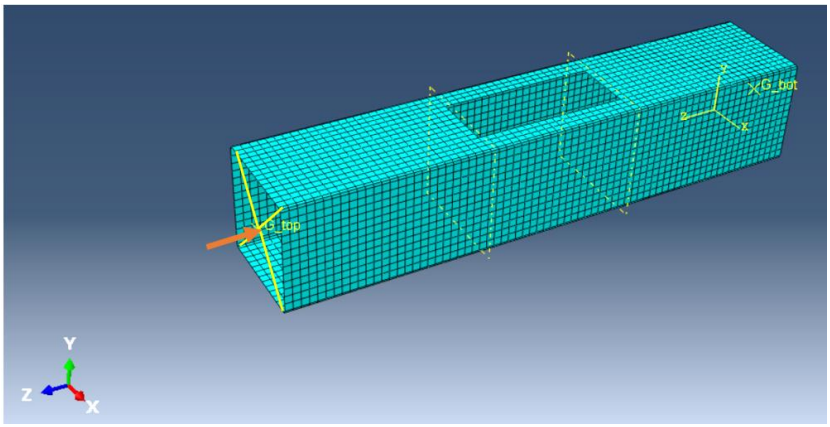

Figure 1: 3D overview of the numerical model

For the GMNIA intended to reach the cross-section resistance, an equivalent local imperfection equal to *h*/400 (*h* is the width of the cross-section) with shape affine to the first local elastic instability mode has been adopted. This value shows a better agreement with the design curve (Winter's curve) for local buckling given in EN 1993-1-5. This assumption is based on the outcomes of the HOLLOSSTAB project where it has been validated through experimental tests and is also in line with research works found in the literature [14]-[15].

For the GMNIA intended to reach the buckling resistance of the member, the following two initial imperfections have been implemented: (i) an equivalent global imperfection equal to *L*/1000 (*L* being the member length) with shape affine to the first global elastic instability mode, and (ii) an equivalent local imperfection equal to *h*/400 as explained above. Again, the selected combination of imperfections is in line with the outcomes of the HOLLOSSTAB project.

In the conducted parametric study, the profiles have been selected in order to cover a wide range of cross-section plate slenderness, while the member lengths were varied so as to account for both local and flexural buckling through the global slenderness range. Subsequently, numerical investigations on short and slender columns subjected to compression, or compression and bending with or without handholes have been performed. For this study, the size of the handholes is assumed to be constant and equal to 140x55 mm.

3 CROSS-SECTION RESISTANCE

For the cross-section resistance, two different configurations have been considered: (i) short columns with gross cross-section in order to validate the numerical tool, and (ii) short columns with a handhole at their mid-height. For sake of simplicity, the section with the handhole will be named hereafter as "net section". For both configurations, the load is implemented at the centre of gravity of the SHS profile, while for the second configuration, an additional loading case has been considered where the load is introduced on one of the column faces as explained in §3.2.3.

3.1 Gross cross-section – validation of FEM

Table 1 presents the details of the cross-sections that have been considered as well as their numerically and analytically determined resistances under pure compression. To prevent

flexural buckling, the length of the samples was selected in such a way that $\bar{\lambda} \leq 0{,}2$, a slenderness below which the European buckling curves assume that no reduction associated to buckling is required. The numerical resistance ($N_{ult,n}$) corresponds to the maximum failure load, while the analytical one may be determined as follows:

$$N_{c,Rd} = \begin{cases} A \cdot f_{yb} & if\ A_{eff} = A \\ A_{eff} \cdot f_{yb} & if\ A_{eff} < A \end{cases} \quad (1)$$

where the effective area is calculated according to EN 1993-1-3 accounting only for local buckling phenomena, as distortion is not relevant for closed sections. Therefore, the buckling factor given in EN 1993-1-5, Table 4.1, is $k_\sigma = 4$ and the reduction factor is $\rho = (\bar{\lambda}_p - 0{,}22)/\bar{\lambda}_p^2$. It can be easily seen that both numerical and analytical resistances are quite similar with a mean value of the ratio $n = N_{ult,n}/N_{c,Rd}$ equal to 1,01 with a CoV of 1,4%.

Table 1: Resistance of gross cross-section subjected to compression

No	Cross-section	L [mm]	$\bar{\lambda}_p$ [-]	ρ [-]	A_{eff} [mm^2]	$N_{c,Rd}$ [kN]	$N_{ult,n}$ [kN]	ρ_{num} [-]	n [-]
1	SHS 140x2	1000	1,584	0,544	590	236,0	236,3	0,540	1,00
2	SHS 140x3	800	1,048	0,754	1216	486,4	494,5	0,763	1,02
3	SHS 140x5	600	0,620	1,000	2636	1054	1039,0	0,986	0,99
4	SHS 120x2	590	1,354	0,618	574	229,4	229,8	0,615	1,00
5	SHS 120x4,5	590	0,589	1,000	2027	810,7	807,5	0,996	1,00
6	SHS 120x5,5	590	0,478	1,000	2441	976,4	994,6	1,019	1,02
7	SHS 100x2	500	1,125	0,715	550	220,2	225,8	0,729	1,03
8	SHS 100x3	500	0,742	0,948	1080	432,1	439,0	0,962	1,02
9	SHS 100x5	500	0,436	1,000	1836	734,2	756,9	1,031	1,03
10	SHS 150x2	500	1,699	0,512	596	238,6	244,7	0,521	1,03
11	SHS 150x3,5	600	0,961	0,802	1614	645,7	670,5	0,830	1,04
12	SHS 150x6	500	0,551	1,000	3363	1345,3	1353,0	1,006	1,01
13	SHS 160x2	640	1,813	0,485	602	240,9	244,0	0,487	1,01
14	SHS 160x3	640	1,201	0,680	1258	503,2	506,3	0,680	1,01
15	SHS 160x4,5	640	0,793	0,911	2498	999,2	1033,0	0,940	1,03

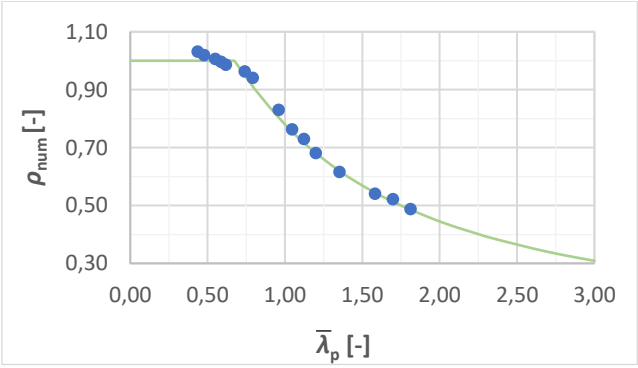

Figure 2: Comparison of the numerical results with the buckling design curve of EN 1993-1-5

Figure 2 presents the numerically determined reduction factor $\rho_{num} = N_{ult,n}/N_{pl}$ versus the plate slenderness (corresponding to the plate slenderness of an internal plate). The very good agreement between the numerical results and the buckling design curve of EN 1993-1-5 can be easily observed. It can be therefore concluded that the numerical model predicts the design resistance of these sections with a high accuracy, while the selected values of the initial imperfections and the material law are suitable.

3.2 Resistance of a cross-section with a handhole

In order to check the resistance of the net section, the same samples as in §3.1 were assumed but with a handhole at their mid-height; two loading cases were also considered.

3.2.1 Case 1: Centrally loaded short columns

Despite the fact that the member is subjected to an axial load at the centre of gravity G of the gross section, at the position of the handhole, a bending moment is appearing due to the eccentricity of the point application of the load (i.e. G) and the centroid of the net and/or the effective section (i.e. G_1 and G_2, see Figure 3). Thus, the net section should be checked against $N_{Ed} + M_{Ed,z}$, and the following formula may be used:

$$\frac{N_{Ed}}{N_{c,Rd}} + \frac{M_{z,Ed}+\Delta M_{z,Ed}}{M_{c,Rd}} \leq 1{,}0 \qquad (2)$$

To compute the design resistances of the net section according to eq.(2), the procedure of EN1993-1-3 is followed, where the upper and the bottom flanges with the edge folds are treated as stiffeners and both local and distortional buckling are accounted for. Local buckling is covered by the provisions of EN 1993-1-5 while distortional buckling by EN 1993-1-3. In addition, according to EN 1993-1-3, the effective cross-sectional aera A_{eff} should be determined by assuming that the cross-section is subjected only to uniform stresses due to axial compression in its centre of gravity G_1, while for the calculation of the effective section modulus W_{eff}, the member is subjected only to bending.

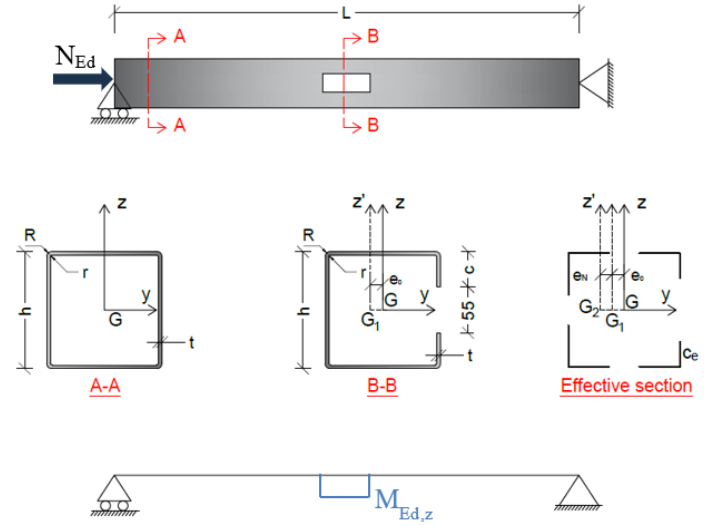

Figure 3: Static system, bending moment diagram and gross, net and effective cross-sections

Figure 4(a) presents (in blue) the ratio of the numerically determined resistance of the net section to its analytical one versus the plate slenderness (corresponding to the plate slenderness of an internal plate). The numerical resistance ($N_{ult,n}$) corresponds to the maximum failure load, while the analytical one (N_{anal}) is derived as the maximum axial load that satisfies eq.(2). The mean value (solid blue line) of the ratio $N_{ult,n}/N_{anal}$ is equal to 1,23 with a CoV (dotted blue line) of 15%. It can be seen that the analytical resistance is always on the safe side, with the most conservative results being for the slenderest sections. It should be mentioned that the analytical resistances have been evaluated with the simplified method that Eurocode follows, where the effective properties are calculated apart for cross-section subjected only to compression and/or only to bending. This method is easier to be applied in practice but the stress distribution used for the calculation is not reflecting the actual one. When the actual stress distribution is used (green points in Figure 4(a)), again the predicted resistances are on the safe side. For low to

intermediate slenderness, the predictions are close to the ones evaluated with the simplified procedure given in EC3, while for the slenderest ones, the consideration of the actual stresses seems to be even more conservative. It can be thus concluded that the simplified procedure given in EN 1993-1-3 provides sufficient and safe results. It should be also mentioned that according to EN 1993-1-3, for profiles where there is no reduction to their area, the value of the average yield strength f_{ya} can be used to determine the resistance instead of the basic one f_{yb}. However, as the majority of considered profiles are thin-walled ones and so are prone to local buckling, the beneficial effect of the use of f_{ya} is negligible; it can be applied only for two of the considered specimens and gives less conservative results almost by 2%.

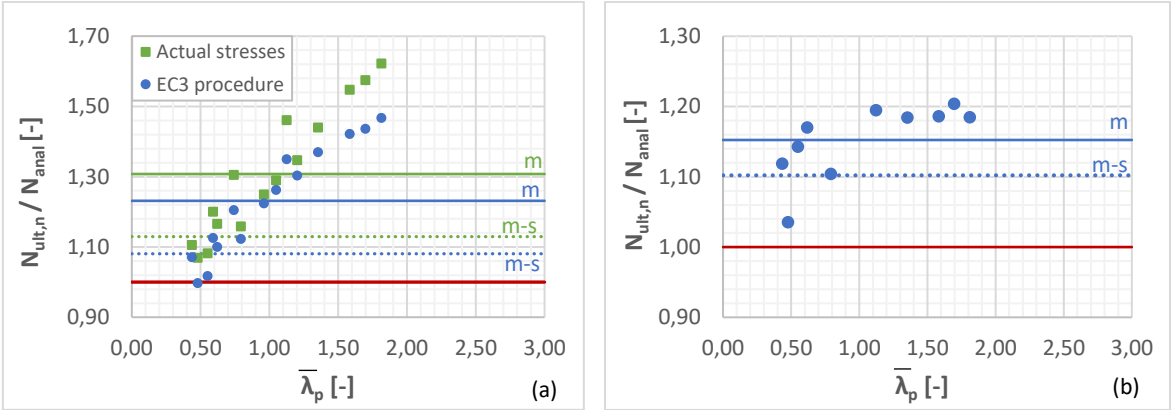

Figure 4: Comparison of the numerical and analytical sectional resistances for (a) case 1 and (b) case 2

3.2.2 Case 2: Eccentrically loaded short columns

Although the beam could be bolted on all the column faces except the one with the handhole, it has been selected here to check the cross-sectional resistance with an eccentricity $e_z = (h\text{-}t)/2$ (see Figure 3 for the axis definition), as an eccentricity in *y* axis is anyway developed due to the net/effective cross-section. For this case, the net section is subjected to axial force and bi-axial bending and so it's resistance should be checked, using the following formula:

$$\frac{N_{Ed}}{N_{c,Rd}} + \frac{M_{y,Ed}}{M_{cy,Rd}} + \frac{M_{z,Ed}+\Delta M_{z,Ed}}{M_{cz,Rd}} \leq 1{,}0 \qquad (3)$$

Figure 4(b) presents the ratio of the numerically determined resistance of the net section to its analytical one, versus the plate slenderness. The numerical resistance corresponds to the maximum failure load, the analytical one is derived as the maximum axial load that satisfies eq.(3), while EN 1993-1-3 was again followed for the calculation of effective sectional properties. Once more, the analytically determined resistance is safe side with a mean value of the ratio $N_{ult,n}/N_{anal}$ equal to 1,12 and a CoV of 4,8 %.

4 CRITICAL BUCKLING LOAD

Given that only the global critical loads are introduced in the design process for the determination of the buckling resistance of the member, while local or/and distortional buckling effects are accounted for through the effective properties of the cross-sections, the investigations are focused here on the influence of the handholes to the flexural critical load; torsional buckling is not deemed to occur in hollow sections. For these numerical and analytical investigations, 10 different profiles with a global slenderness varying from 0,599 to 2,074 have been contemplated with five different member layouts as they are illustrated in Figure 5. The case where no handholes have been assumed along the member aims first to validate the

software, and secondly, is used as the reference value with which all the critical loads obtained for the members with handholes are compared.

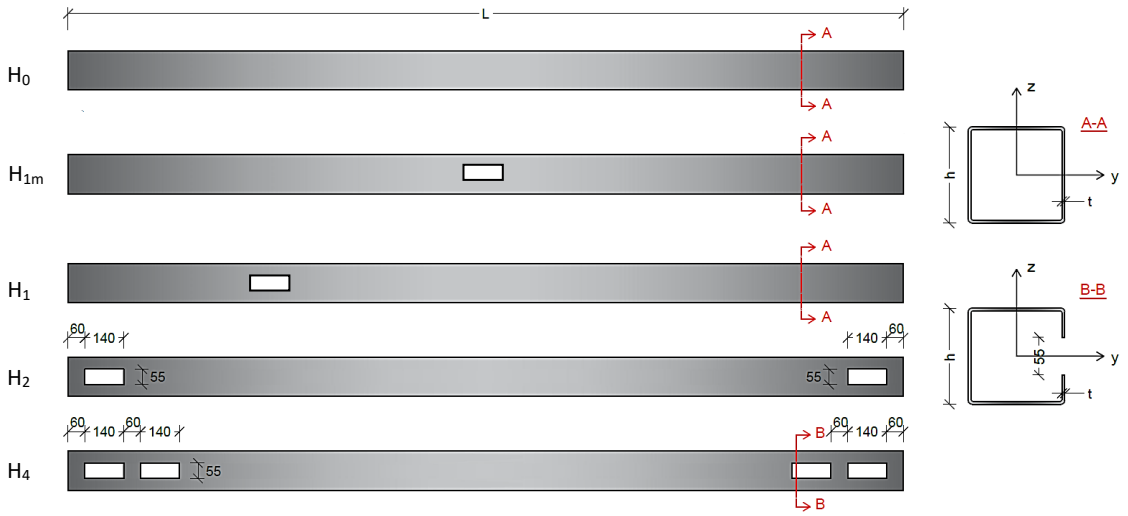

Figure 5: Layout, geometry details and notations of the studied members

Due to lack of space, the tables with the resulted values are omitted and only the main conclusions related to this study are presented here. First of all, both numerical and analytical critical loads for members with gross SHS are quite similar (differences between 0-2%). The position of the handhole affects the critical load, with the biggest impact being when the hole is at the mid-heigh of the member and the less at its extremities. In addition, due to the presence of the handholes along the member's length, there is no more a pure flexural buckling mode but a combination of flexural buckling with a slight presence of local buckling around the holes. Although this local buckling is more pronounced in $N_{cr,n,y}$ than in $N_{cr,n,z}$ (critical loads along y and z axis respectively – see Figure 5 for the definition of the axis in regard to the position of the handhole), it is however remaining rather limited. Finally, the existence of the handholes at the extremities reduces the critical load by 1-3% compared to the gross cross-section flexural critical load. This difference seems as rather small and its impact on the ultimate buckling resistance of the member is negligible.

5 BUCKLING RESISTANCE

As previously, the numerical model is first validated through cases where members with gross SHS sections are subjected to pure compression and then, the influence of the handholes at the member's extremities on the ultimate buckling resistance is investigated.

5.1 Gross cross-section – validation of FEM

Table 2 presents the details of the samples that have been considered as well as their numerically and analytically determined buckling resistances to pure compression. The samples have been selected so as to cover a wide range of member slenderness where both local and global instabilities are relevant. The analytical resistance is given by the expression:

$$N_{b,Rd} = \begin{cases} \chi \cdot A \cdot \frac{f_{yb}}{\gamma_{M1}} & if\ A_{eff} = A \\ \chi \cdot A_{eff} \cdot \frac{f_{yb}}{\gamma_{M1}} & if\ A_{eff} < A \end{cases} \quad (4)$$

where the effective properties are calculated according to EN 1993-1-3. The value of the buckling reduction factor χ is computed by using buckling curve b in combination with the

basic yield stress f_{yb} according to EN 1993-1-3. The use of buckling curve *b* is in line with the recommendations of the CIDECT [16], is on the safe side compared to buckling curve *a* that has been justified in HOLLOSSTAB project and is less conservative according to EN 1993-1-1 where buckling curve *c* is proposed for cold-formed sections.

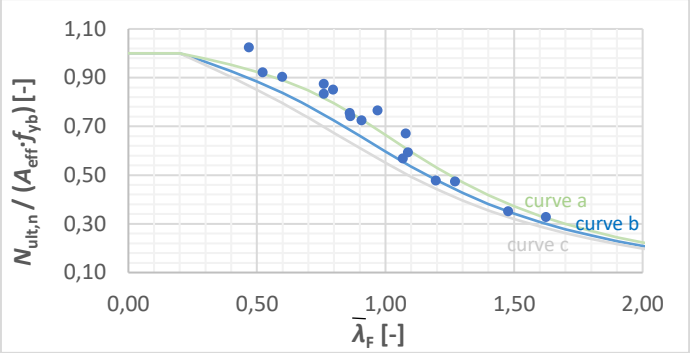

Figure 6: Comparison of the numerical results with the buckling curves of EN 1993-1-1

It can be easily seen from Table 2 that there is a good agreement between the numerical results and the ones calculated according to EN 1993-1-3, with the code provisions being always on the safe side; the mean value of the ratio $n = N_{ult,n}/N_{b,Rd}$ is equal to 1,10 with a deviation of 6,7%. Figure 6 shows the numerically determined reduction factor $\chi_{num} = N_{ult,n}/(A_{eff} \cdot f_{yb})$ versus the global flexural slenderness; the buckling curves given in EN 1993-1-1 are illustrated too. It can be observed that all the results are above curve *b*. Subsequently, the numerical model appropriately predicts the buckling resistance of members with SHS gross sections, while the selected values for the initial imperfections, the material law and the buckling curve are justified.

Table 2: Buckling resistance of gross cross-section subjected to compression

No	Cross-section	L [mm]	$N_{cr,F}$ [kN]	$N_{cr,local}$ [kN]	$\bar{\lambda}_p$ [-]	$\bar{\lambda}_F$ [-]	χ [-]	$N_{b,Rd}$ [kN]	$N_{ult,n}$ [kN]	n [-]
1	SHS 140x2	5000	286,4	174,4	1,58	0,91	0,656	154,9	170,9	1,10
2	SHS 140x2	7000	146,1	174,4	1,58	1,27	0,441	104,1	111,5	1,07
3	SHS 140x3	4000	652,1	590,1	1,05	0,86	0,684	332,9	360,8	1,08
4	SHS 140x3	5000	417,4	590,1	1,05	1,08	0,548	266,3	326,1	1,22
5	SHS 140x5	3000	1821,9	2744,8	0,62	0,76	0,748	789,0	921,4	1,17
6	SHS 120x2	3800	309,3	203,6	1,35	0,86	0,686	157,4	173,1	1,10
7	SHS 120x2	4800	193,8	203,6	1,35	1,09	0,543	124,5	136,1	1,09
8	SHS 120x5,5	2000	2722,7	4276,2	0,48	0,60	0,838	817,9	881,0	1,08
9	SHS 100x2	3300	234,1	244,6	1,13	0,97	0,616	135,7	168,3	1,24
10	SHS 100x5	1300	3331,9	3860,4	0,44	0,47	0,898	659,0	751,9	1,14
11	SHS 100x5	4500	278,1	3860,4	0,44	1,63	0,300	220,3	240,3	1,09
12	SHS 150x2	6500	209,3	162,7	1,70	1,07	0,555	132,4	135,6	1,02
13	SHS 150x2	9000	109,2	162,7	1,70	1,48	0,350	83,6	83,8	1,00
14	SHS 150x6	3200	2321,8	4433,0	0,55	0,76	0,748	1006,4	1121,0	1,11
15	SHS 150x6	2200	4912,2	4433,0	0,55	0,52	0,874	1175,4	1239,4	1,05
16	SHS 160x2	8000	168,2	152,5	1,81	1,20	0,480	115,6	115,8	1,00
17	SHS 160x4,5	3800	1574,1	1746,4	0,79	0,80	0,726	725,9	850,1	1,17

5.2 Buckling resistance of a member with handholes

In order to check the influence of the handholes on the buckling resistance of these members, the same samples reported in Table 2 were considered, and for each member, two configurations have been adopted: members with 1 handhole per extremity and members with 2 handholes per extremity (see Figure 5). Again, in terms of loading, two cases are distinguished: centrally and eccentrically loaded columns.

5.2.1 Case 1: Centrally loaded columns

Figure 7 (a) compares the ultimate buckling resistance of the members with handholes (1 or 2 holes at each extremity) to the numerical resistance of the same members but without handholes, versus their global flexural slenderness. The comparisons are limited to slenderness higher than 0,7 where a member failure occurs, as for lower slenderness the specimen reaches the cross-sectional resistance of the net section. As it is shown, the influence of the handholes on the buckling resistance of the member is limited (differences less than 6%). Figure 7(b) presents the ratio of the numerically determined resistance of the member to its analytical one versus the global flexural slenderness. The analytical resistance is $N_{anal} = \min\{N_{b,Rd}, N_{c,Rd}\}$, where $N_{b,Rd}$ is given by (eq.(4)) and $N_{c,Rd}$ is the resistance of the net cross-section as explained in §3.2.1. The mean value of the ratio $N_{ult,n}/N_{anal}$ is equal to 1,12 and 1,11 for specimens with 1 hole/extremity and 2 holes/extremity respectively; CoV is 8,6% and 8,8% correspondingly. Furthermore, the analytically determined resistance is on the safe side for all specimens.

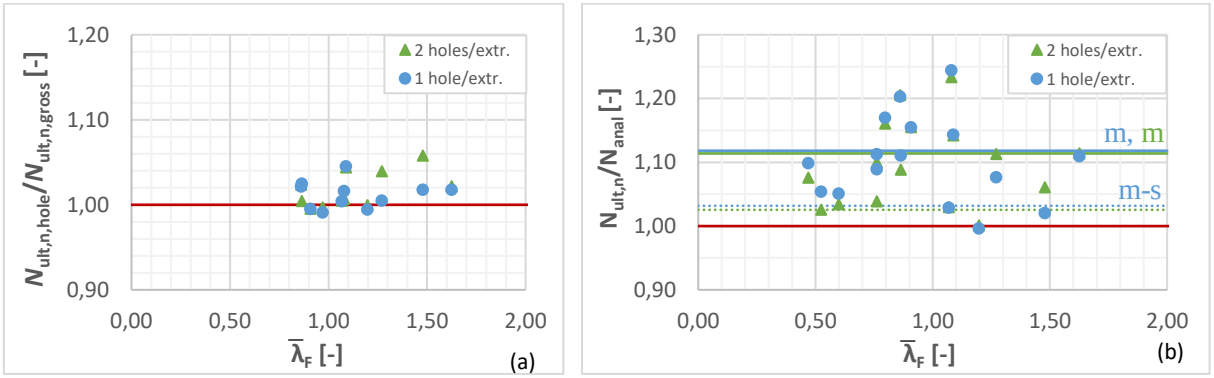

Figure 7: (a) Comparison of the numerical resistances for members with and without handholes and (b) Comparison of the numerical and analytical buckling resistances (Case 1)

5.2.2 Case 2: Eccentrically loaded columns

As in §3.2.2, the load is introduced with an eccentricity $e_z = (h\text{-}t)/2$. It has been found for this loading case too that the influence of the handholes to the buckling resistance of the member is limited (differences less than 3%). Figure 8 presents the ratio of the numerically determined resistance of the member to its analytical one versus the global flexural slenderness. The analytical resistance is $N_{anal} = \min\{N_{b,Rd}, N_{c,Rd}\}$, where $N_{b,Rd}$ is determined for the member without accounting for the handholes in accordance with EN 1993-1-3-§6.5.2 and by applying method 2 for the k_{ij} interaction factors as the profile is not susceptible to torsional deformations, while $N_{c,Rd}$ is the resistance of the net cross-section as explained in §3.2.2. For both configurations of handholes, the mean value of the ratio $N_{ult,n}/N_{anal}$ is equal to 1,10 with a CoV of 4,2% and 4,9% for specimens with 1 hole/extremity and 2 holes/extremity respectively. As it has been demonstrated, the analytically determined resistance is on the safe side for all specimens. Although alternative formulae are provided in prEN 1993-1-3 for this case, their validity is not checked in this paper.

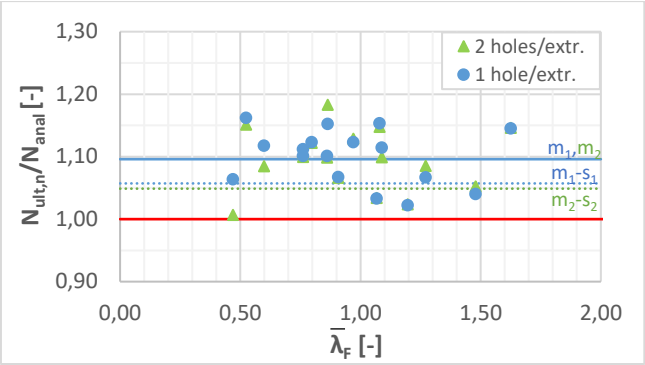

Figure 8: Comparison of the numerical and analytical buckling resistances (Case 2)

6 CONCLUSION

This paper investigates the influence of large holes used at the extremities of SHS thin-walled columns for tightening the bolts by hand, on their resistance and stability. More specifically, the behaviour of these elements has been studied numerically using shell elements, accounting for both local and distortional effects, as well as material and geometrical non-linearities. Then, the obtained results have been compared with the provisions of EN 1993-1-3. Through this study, the following recommendations for the practitioners may be drawn:

- the current version of EN 1993-1-3 can be safely used to calculate the resistance of columns with handholes;
- for the cross-section where the handhole is located, both local and distortional effects should be taken into account in the prediction of its resistance according to EN1993-1-3;
- the handholes at the extremities are slightly affecting the critical buckling load of the column, but the impact on the ultimate resistance is limited;
- the handholes may be neglected in the buckling design resistance of the member.

REFERENCES

[1] Toffolon, A., Müller, A., Niko, I., Taras, A., 'Experimental and numerical analysis of the local and interactive buckling behaviour of hollow sections', *Proceedings of the 14th Nordic Steel Construction Conference (NORDIC STEEL 2019)*, Copenhagen, Denmark, 2019.

[2] Toffolon, A., Taras, A., 'Proposal of a design curve for the overall resistance of cold formed RHS and SHS members', *Proceedings of the 14th Nordic Steel Construction Conference (NORDIC STEEL 2019)*, Copenhagen, Denmark, 2019.

[3] Yun, X., Meng, X., Gardner, L., 'Design of cold-formed steel SHS and RHS beam–columns considering the influence of steel grade', *Thin-walled Structures*, 171, 108600, 2022.

[4] Li, S.H., Zeng, G., Ma, Y.F., Guo, Y.J., Lai, X.M., 'Residual stresses in roll-formed square hollow sections', *Thin-walled Structures*, 47, 505-513, 2009.

[5] HOLLOSTAB: Overall-Slenderness Based Direct Design for Strength and Stability of Innovative Hollow Sections, *Research Program of the Research Fund for Coal and Steel*, Grant Agreement Number:RFCS-2015-709892.

[6] Singh, T., Chan, T.-M., 'Effect of access openings on the buckling performance of square hollow section module stub columns', *Journal of Constructional Steel Research*, 177, 106438, 2021.

[7] Devi, S., Singh, T., Singh, K., 'Cold-formed steel square hollow members with circular perforations subjected to torsion', *Journal of Constructional Steel Research*, 162, 105730, 2019.

[8] ABAQUS, User's manual, Version 6.14, Simulia, 2014.

[9] *EN 1993-1-3. Eurocode 3: Design of steel structures - Part 1-3: General rules - Supplementary rules for cold-formed members and sheeting*, Brussels, Comité Europeen de Normalisation, 2006.

[10] *EN 1993-1-1: Design of steel structures - Part 1-1: General rules and rules for buildings*, Brussels, Comité Européen de Normalisation, 2005.

[11] *EN 1993-1-5: Design of steel structures - Part 1-5: Plate structural elements*, Brussels, Comité Europeen de Normalisation, 2006.

[12] *prEN 1993-1-3. Eurocode 3: Design of steel structures - Part 1-3: General rules - Supplementary rules for cold-formed members and sheeting*, Brussels, Comité Europeen de Normalisation, 2020.

[13] *EN10346: Continuously hot-dip coated steel flat products - Technical delivery conditions*, Brussels, Comité Européen de Normalisation, 2009.

[14] Muller, A., Vild, M., Taras, A., 'Decision tree for local + global imperfection combinations in double-symmetric prismatic members', *Steel Construction*, 16, 2-15, 2023.

[15] Rusch, A., Lindner, J., 'Überprüfung der grenz (b/t)-Werte für das Verfahren Elastisch-Plastisch', *Stahlbau*, 70, 857-868, 2001.

[16] Rondal, J., Wurker, K.-G., Dutta, D., Wardenier, J., Yeomans, N., 'Structural stability of hollow sections' (book), CIDECT, *Construction with hollow sections, Verlag TUV Rheinland GmbH*, Koln, Germany, ISBN:3-8249-0075-0, 1992.